Pergamon

0956-7151(94)00481-1

Acta metall. mater. Vol. 43, No. 8, pp. 3001–3007, 1995
Elsevier Science Ltd

0956-7151/95 $9.50 + 0.00

DEFORMATION AND FAILURE OF A CARBON FIBRE COMPOSITE UNDER COMBINED SHEAR AND TRANSVERSE LOADING

N. A. FLECK and P. M. JELF

Department of Engineering, University of Cambridge, Trumpington Street, Cambridge CB2 1PZ, England

(Received 3 August 1994; in revised form 3 December 1994)

Abstract—The in-plane shear and transverse properties are measured for T800-924C carbon fibre reinforced epoxy unidirectional material. Non-linearity in the shear response is ascribed partly to plasticity and partly to micro-crack growth within the matrix. The stress–strain response under proportional and non-proportional stressing supports the use of a deformation theory of plasticity. A failure envelope is measured and presented in both stress space and in strain space for the composite; failure is associated with distributed tensile micro-cracking within the matrix.

1. INTRODUCTION

Compressive failure by plastic microbuckling is a design limiting feature of long-fibre polymer–matrix composites, as shown in Fig. 1(a). Microbuckling is a plastic instability, and occurs within a well-defined band, of width 10–20 fibre diameters, by the rotation of fibres within the band. Fibre rotation induces both in-plane transverse and shear straining of the composite [1]. The transverse component of straining is thought to involve distributed micro-cracking and distributed micro-voiding within the epoxy matrix, as shown by the micrograph of a microbuckle in Fig. 1(b).

The aim of the current paper is to validate experimentally the constitutive relations previously assumed in microbuckling analysis for combined shear and transverse loading. A yield surface and a failure surface are obtained, and failure mechanisms are examined. The in-plane response of fibre composites to proportional and non-proportional loading is also of basic interest to the overall mechanical behaviour of laminated composites.

Conventionally, in-plane properties are measured from tests on circumferentially wound tubes: this raises the concern as to whether the processing route for hoop wound tubes gives properties which are representative of those for autoclaved laminated pre-preg. In the present study, the difficulty is overcome by hoop winding pre-preg material over a mandrel, prior to autoclaving.

An alternative method of determination of in-plane properties is to subject flat laminated plates to uniaxial tension; the fibre direction in each lamina is inclined at a finite angle $\pm\theta$ about the loading direction. Thus, the ratio of transverse strain to shear strain is set by the fibre inclination angle θ. The obvious drawbacks with this test method are the free edge effects and the difficulty of applying non-proportional loading such that the ratio of transverse stress to shear stress changes during a test.

2. REVIEW OF CONSTITUTIVE LAW USED IN PLASTIC MICROBUCKLING THEORY

Budiansky and Fleck [1] have analysed in some depth the un-notched compressive strength of fibre composites due to plastic microbuckling. They assume that microbuckling is by the rotation of inextensional fibres within a band as shown in Fig. 1(a); material within the band undergoes non-proportional transverse and shear straining on axes which rotate with the fibres as shown in Fig. 1(a).

For the case of an elastic–perfectly plastic composite response, Budiansky and Fleck [1] assume that the shear stress τ and transverse stress σ_T satisfy a yield condition of elliptical shape

$$(\tau/\tau_y)^2 + (\sigma_T/\sigma_{Ty})^2 = 1 \qquad (1)$$

where τ_y and σ_{Ty} are the yield strengths in pure shear and pure transverse tension, respectively. For the more representative case of a strain hardening material, equation (1) may be generalised by defining an effective stress, τ_e via

$$\tau_e^2 = \tau^2 + \frac{\sigma_{Ty}^2}{R^2}. \qquad (2)$$

The constant R defines the eccentricity of the yield ellipse, and is given by the ratio of the yield stresses

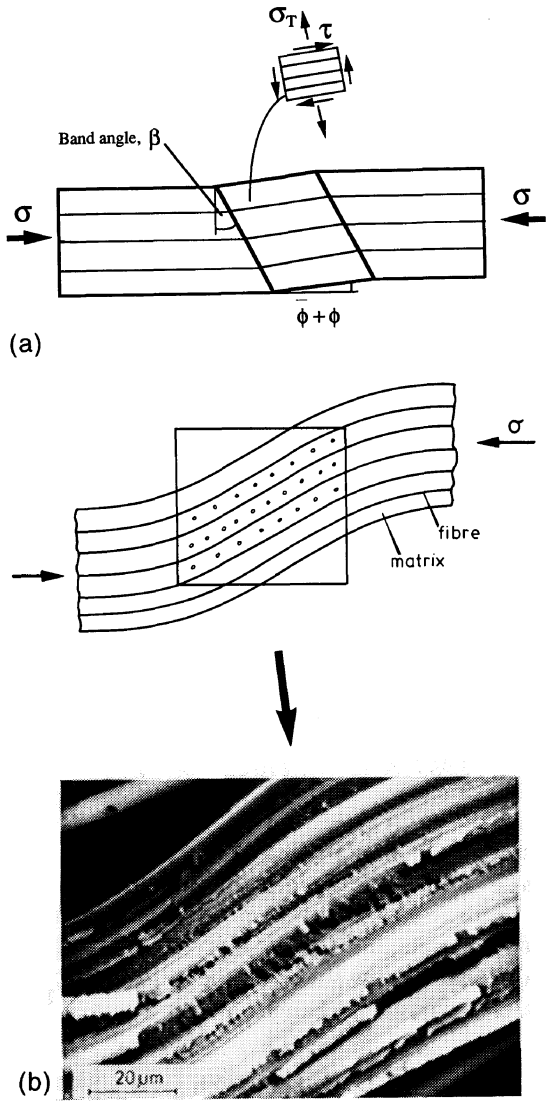

Fig. 1. (a) Idealised microbuckle, inclined at an angle β to the fibre direction. The fibres have an initial uniform misalignment $\bar{\phi}$ within the band, and rotate through an additional angle ϕ under the remote axial stress σ. (b) *In situ* scanning electron micrograph of a microbuckle band under load. The epoxy matrix has dilated due to distributed micro-cracking.

in pure tension and shear, $R \equiv \sigma_{Ty}/\tau_y$. Budiansky and Fleck [1] consider a deformation theory version of plasticity whereby the total shear strain γ and the total transverse strain ϵ_T depend only upon the shear stress τ and the transverse stress σ_T. An effective strain γ_e is introduced in terms of the shear strain γ and the transverse strain ϵ_T

$$\gamma_e^2 = \gamma^2 + R^2\epsilon_T^2 \tag{3}$$

and the functional dependence of γ_e upon τ_e is taken to be the same as that of γ upon τ in a shear test. If in a simple shear test we define the secant modulus G_s by $G_s(\tau) \equiv \tau/\gamma$ and the tangent modulus G_t by $G_t(\tau) \equiv \dot{\tau}/\dot{\gamma}$, then the effective shear stress τ_e is related to γ_e by $G_s(\tau_e) = \tau_e/\gamma_e$ and $G_t(\tau_e) = \dot{\tau}_e/\dot{\gamma}_e$.

Following the usual assumption that the direction of the strain vector (γ, ϵ_T) is normal to the contour of constant τ_e in (τ, σ_T) space, the total strain components γ and ϵ_T are given by

$$\gamma = \frac{\tau}{\tau_e}\gamma_e \tag{4a}$$

and

$$\epsilon_T = \frac{\sigma_T}{R^2\tau_e}\gamma_e. \tag{4b}$$

The incremental stress–strain response is derived by differentiation of above relations, giving

$$\dot{\gamma} = \frac{\dot{\tau}}{G_s} + \left(\frac{1}{G_t} - \frac{1}{G_s}\right)\frac{\tau\dot{\tau}_e}{\tau_e} \tag{5a}$$

$$\dot{\epsilon}_T = \frac{\dot{\sigma}_T}{R^2G_s} + \left(\frac{1}{G_t} - \frac{1}{G_s}\right)\frac{\sigma_T\dot{\tau}_e}{R^2\tau_e} \tag{5b}$$

where

$$\dot{\tau}_e = \frac{\tau\dot{\tau}}{\tau_e} + \frac{\sigma_T\dot{\sigma}_T}{R^2\tau_e}. \tag{5c}$$

It remains to state a strain hardening law. Budiansky and Fleck [1] assume a Ramberg–Osgood relation between γ_e and τ_e

$$\frac{\gamma_e}{\gamma_y} = \frac{\tau_e}{\tau_y} + \frac{3}{7}\left(\frac{\tau_e}{\tau_y}\right)^n \tag{6}$$

in terms of the three material parameters τ_y, γ_y and n. For the case of pure shear loading, τ_e reduces to τ and γ_e reduced to γ. The material parameters are determined from the τ vs γ pure shear response by the following strategy.

(i) The initial slope $d\tau/d\gamma = \tau_y/\gamma_y = G$, where G is the elastic shear modulus
(ii) A secant line is drawn from the origin of slope $7G/10$. It intersects the τ vs γ plot at $\tau = \tau_y$, $\gamma = 10\gamma_y/7$. This procedure gives values for τ_y and γ_y.
(iii) Calculate a value for the strain hardening index n by fitting relation (6) to a point of the τ vs γ plot, at a value of γ equal to several times γ_y. Alternatively, a least squares fit can be used to determine n.

Budiansky [2] has shown that a deformation theory version of plasticity is physically meaningful for the yielding of metals when loading is close to proportional. When loading is far from proportional flow theory is more accurate. Over short time scales it is thought that the non-linear visco-elastic flow of toughened epoxy can be modelled adequately by plasticity theory. Indeed, there has been considerable previous success in characterising the yield behaviour of thermoplastics and thermosetting plastics in terms of plasticity theory; see for example, the review by Ward [3]. A thrust of the current paper is to give support for the use of a simple plasticity theory in the yielding of carbon fibre–epoxy composites.

Budiansky and Fleck [1] assume that plane strain deformation occurs within a microbuckle band as the width of the band is taken to be much less than the thickness of the material. Thus the volumetric strain within the band equals the transverse strain ϵ_T, and the above plasticity theory is dilatant in nature.

It has proved difficult to obtain in-plane material properties under strict plane strain conditions, i.e. with zero prescribed normal strain. The authors have attempted to obtain plane strain material data by testing circumferentially wound tubes containing an external circumferential deep notch. These experiments were not successful as brittle fracture intervened from the notch root prior to constrained plastic flow. The current experimental study is limited to plane stress data, where the stresses normal to the plane of the composite sheet are negligible.

3. EXPERIMENTAL METHOD

3.1. Specimen preparation

The composite system examined in this work consisted of Toray T800 carbon fibres in a Ciba-Geigy 924c toughened epoxy matrix. The composite tubes were manufactured by hoop winding pre-preg sheet around a circular section mandrel, followed by a cure cycle 150°C for 4 h at ambient atmospheric pressure. The tubes were wound with shrink-wrap tape in order to aid consolidation. It should be noted that this is not the cure procedure recommended for T800/924 material. The tube material was therefore not fully consolidated.

The specimen geometry is shown in Fig. 2(a). The tube is of 25.4 mm o.d. and has an approximate wall thickness of 2 mm. Specimens were cut to a length of 90 mm and mounted on a tapered mandrel to allow the outside diameter to be ground concentrically to the bore. The waisted profile was cylindrically ground to a wall thickness of 1 mm in the gauge section.

3.2. Test methods

The test fixture is given in Fig. 2(b). The upper part of the tubular specimens was attached to the torsion-head by a split collar arrangement. The lower gripped section of tube was adhesively bonded into a cup attached to the lower axial cross-head. This procedure eliminated any bending effects due to grip misalignment. Since the tubes are hoop-wound, axial loading of the tube generates direct stress in the direction transverse to the fibre direction: the in-plane transverse stress σ_T equals the average axial stress in the wall of the tubes. Torsional loading of the tubes gives rise to an in-plane shear stress τ.

The strain response was recorded using thin foil strain gauges adhesively bonded to the specimen. Strain gauge rosettes were employed such that 3 mm long gauges were arranged axially (0°) and at +45°

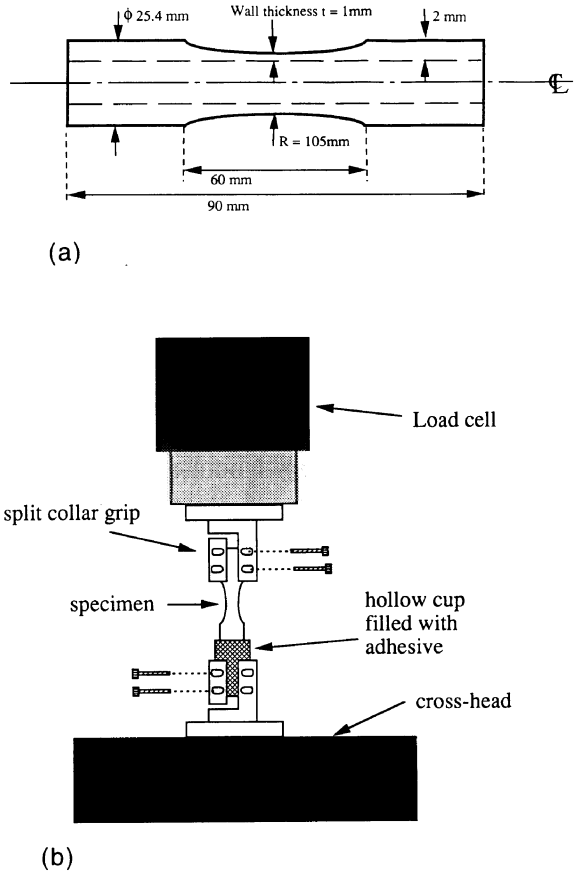

Fig. 2. (a) Specimen design; (b) test fixture.

and −45° to the axial direction. The gauges were attached to the exterior of the tube at the centre of the waisted section. Additional gauges were placed around the circumference of the specimens to confirm that bending effects were negligible. Strain, torque and axial load were recorded at regular intervals throughout each test using a computerised data-logging system.

Tests were conducted in load control and in torque control, such that the average axial strain rate and average shear strain rate during a test were $10^{-4}\,s^{-1}$. Two types of tests were used to explore the material response: proportional loading and non-proportional loading. In the proportional loading tests the ratio of shear stress τ to transverse stress σ_T was held constant; these tests included the limiting cases of pure shear, pure axial compression and pure axial tension. In the non-proportional loading tests the ratio of shear to axial loading was varied during the test.

4. RESULTS

4.1. Proportional loading tests

In the proportional loading tests, the ratio of transverse stress σ_T to shear stress τ was held constant during each test. The relative proportion of σ_T and τ ranged from pure transverse tension through pure shear to pure transverse compression; results

Table 1. Results of the proportional loading tests

Ratio of transverse stress to shear stress σ_T/τ	0.01% Offset shear stress (MPa)	0.05% Offset shear stress (MPa)	Fracture shear stress (MPa)	0.01% Offset transverse stress (MPa)	0.05% Offset transverse stress (MPa)	Fracture transverse stress (MPa)
Transverse tension	—	—	—	21.2	—	36
Transverse compression	—	—	—	22.6	50	130
0	8	21.4	65	—	—	—
1.01	8.1	12.6	28.2	16	—	28.7
3.5	5.5	8.5	8.6	18.1	—	28.3
−1.8	17	27.4	71	12.9	43	127

are given in Table 1. Yield stresses were determined through the use of 0.01 and 0.05% offset proof strains based on the initial tangent modulus.

The transverse tension and transverse compression responses are shown in Fig. 3(a), and the pure shear response is plotted in Fig. 3(b). In both the transverse loading tests and the shear test, loading was interrupted intermittently and the specimens were unloaded and re-loaded. The purpose of this test sequence was to determine whether non-linearity in response was due to irreversible plasticity (including creep) or a non-linear elastic effect. Examples of this are given in Fig. 3(b) for the case of shear loading. The transverse tensile response was linear to failure (at a failure strain of 0.5%), and unloading–reloading gave a linear elastic response along the same line in stress–strain space as the initial loading trajectory. Slight non-linearity was observed in transverse compression test, see Fig. 3(a). Unloading and reloading of the specimen gave a non-linear elastic response along the initial stress–strain path; the unloading curves are not included for the sake of clarity. The shear test was interrupted when the shear stress τ attained a value of $\tau = 20$ MPa, and again when $\tau = 40$ MPa and $\tau = 60$ MPa. Unloading and reloading to $\tau = 20$ MPa gave a linear elastic response along the original stress–strain path. Unloading and reloading to $\tau = 40$ MPa and to $\tau = 60$ MPa gave a response which was intermediate between that of a non-linear elastic solid (i.e. unloading along the initial loading path without hysteresis) and that of a dissipative solid (unloading with hysteresis).

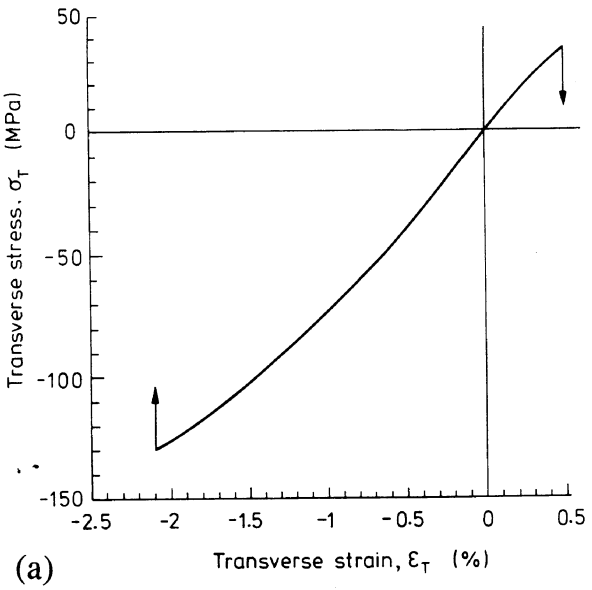

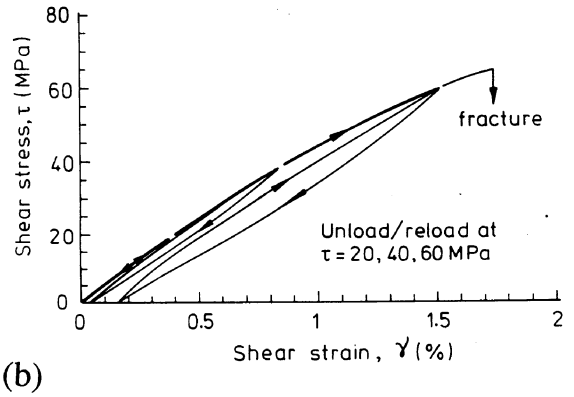

Fig. 3. (a) Transverse tension and compression response; (b) shear response.

It is thought that the non-linear response in compression and in shear is due to a combination of plasticity (including non-linear visco-elasticity) within the toughened epoxy matrix, and micro-cracking within the matrix. Distributed micro-cracking is evident on the fracture surface of all specimens tested to failure: see Fig. 4 for representative fracture surfaces in transverse tension, transverse compression and pure shear. The fracture surfaces also display broken fibres: the fibres are not perfectly aligned in the hoop direction of the tubes, and some fibre fracture is required in order to form a contiguous failure plane. The failure plane was oriented normal to the axis of the tubes in the case of transverse tension and shear. For the case of transverse compression, the failure plane was approximately at 45° to the axis of the tube, on a plane of maximum shear within the matrix.

The results of a typical proportional mixed mode test are shown in Fig. 5(a,b). This test was conducted with a fixed transverse stress–shear stress ratio σ_T/τ of 3.5. The response was slightly non-linear prior to failure at a shear strain of 0.16% and a transverse tensile strain of 0.34%. The plasticity theory presented by Budiansky and Fleck [1] suggests that proportional loading data can be rationalised onto a single "Master Curve" of equivalent shear

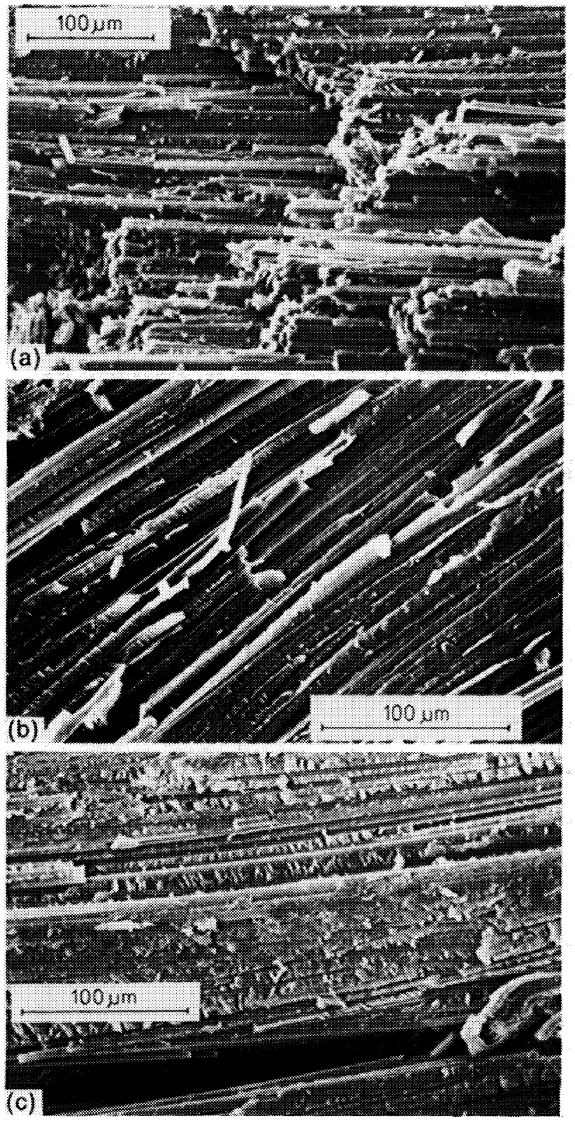

Fig. 4. Scanning electron micrographs of failure surface, tested in (a) transverse tension, (b) transverse compression, and (c) shear.

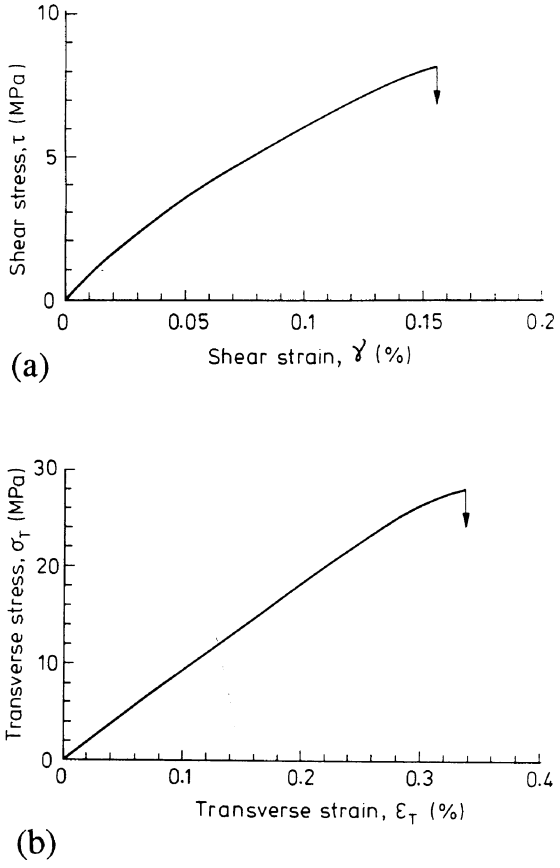

Fig. 5. Typical results for a proportional loading test, with $\sigma_T/\tau = 3.5$. (a) Shear stress τ vs shear strain γ; (b) transverse tensile stress σ_T vs transverse tensile strain ϵ_T.

stress τ_e vs equivalent shear strain γ_e. This has been achieved for the current data by choosing a best fitting value for the material parameter $R = 1.25$, see Fig. 6. [Best fitting values for the Ramberg–Osgood parameters of relation (6) are $\tau_y = 60$ MPa, $\gamma_y = 1.0\%$ and $n = 4.5$.]

Sun and co-workers [4, 5] have developed a similar plasticity theory to that embraced in relations (1)–(5). They have measured the in-plane response of polymer matrix and metal matrix composites by testing $\pm\theta$ laminates. In the terminology of relation (2) above, they find $R = 1.6$ for an AS/3501-5 carbon fibre–epoxy laminate, $R = 1.7$ for an AS4-Peek composite and $R = 2$ for a boron fibre–aluminium composite. The observed value of $R = 1.25$ for correlating the combined loading data of the current study is in good agreement with the measurements of Sun and Chen [4] for polymer matrix composites.

It appears that the plasticity theory encapsulated by equations (1)–(5) is adequate for correlating the strain hardening response under combined loading, but is less able to correlate the failure response of the material. This is further addressed in Fig. 7, which shows the failure surface in both stress space and strain space, for the combined loading tests. The yield surface in (σ_T, τ) space is roughly elliptical in shape and is in fair agreement with the shape given by equation (2), with $R = 1.25$. In contrast the failure surface is highly distorted, with much greater failure strengths under combined transverse compression and shear than under combined tension and shear.

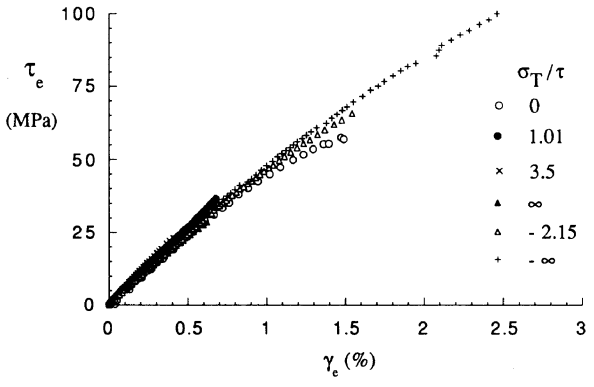

Fig. 6. Normalisation of the proportional loading data to bring the response onto a single master curve of equivalent shear stress τ_e vs equivalent shear strain γ_e. Data are brought together by assuming $R = 1.25$.

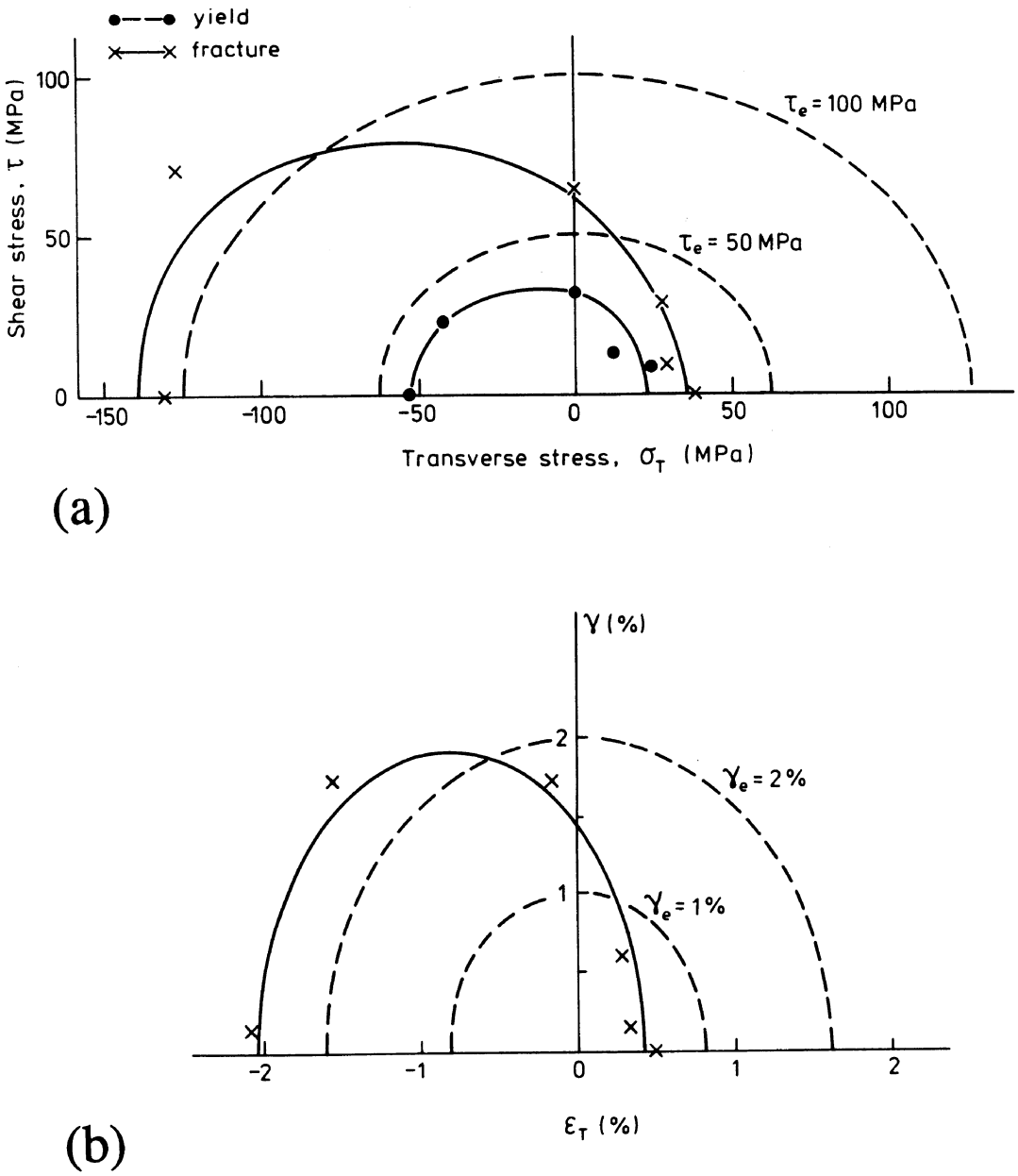

Fig. 7. (a) Yield surface and failure surface in stress space. Yield is taken to occur when 0.05% offset is attained in the shear response. Contours of constant equivalent shear stress τ_e have been added to the plot. (b) Fracture strain in strain space. Contours of constant equivalent shear strain γ_e are included in the plot.

The failure locus is somewhat reminiscent of the failure surface for a soil: the strength is strongly sensitive to the component of hydrostatic stress. The failure envelope is plotted in strain space in Fig. 7(b): the shape resembles that in stress space. Failure occurs soon after yield when the ratio of σ_T/τ is large; when σ_T/τ is small or negative substantial strain hardening occurs prior to fracture.

4.2. Non-proportional loading tests

Three non-proportional loading tests were conducted:

(i) a specimen was loaded in transverse tension, with occasional loading–unloading excursions in shear over a stress range $\Delta\tau = 20$ MPa;

(ii) a specimen was loaded in transverse compression, with occasional loading–unloading excursions in shear over a stress range $\Delta\tau = 20$ MPa; and

(iii) a specimen was loaded in shear, with occasional loading–unloading excursions in transverse tension over a stress range $\Delta\sigma_T = 10$ MPa.

In tests (i) and (ii) the transverse and shear responses were linear, and the tangent moduli were equal to that of the initial elastic values. We omit further details for the sake of brevity. Results for test (iii) are given in Fig. 8. The shear test was interrupted at values for τ of approx. 0, 20, 40 and 60 MPa, and the current yield surface of the tube was probed by applying a transverse tension

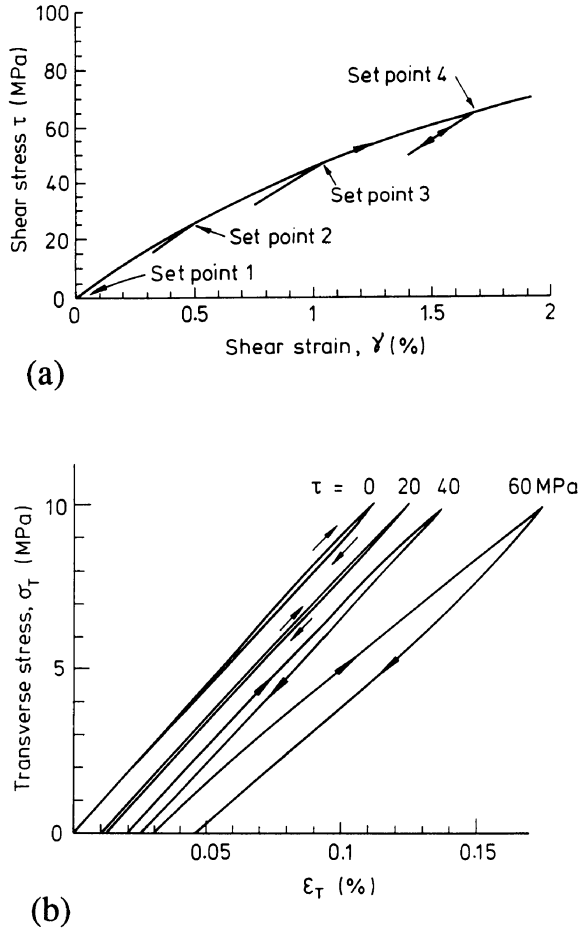

Fig. 8. Non-proportional loading test. The primary loading path is shear, with occasional loading and unloading in transverse tension. (a) Shear response; (b) transverse response.

loading–unloading cycle of range $\Delta\sigma_T = 10$ MPa. The transverse tangent modulus $\dot{\sigma}_T/\dot{\epsilon}_T$ was observed to decrease with increasing torsional pre-loading, see Fig. 8(b).

The instantaneous transverse tangent modulus $\dot{\sigma}_T/\dot{\epsilon}_T$ can also be predicted from the deformation theory of Budiansky and Fleck [1]. Upon specialising equation (5b) for the case of instantaneous transverse loading after pre-loading in shear, we find via equation (5c)

$$\dot{\epsilon}_T = \frac{\dot{\sigma}_T}{R^2 G_s} + \left(\frac{1}{G_t} - \frac{1}{G_s}\right)\frac{\sigma_T^2 \dot{\sigma}_T}{R^4 \tau_e^2}. \qquad (7)$$

The prediction (7) is compared with the experimental data in Fig. 9: we conclude that the deformation theory version (7) is in much better agreement with the experimental data than a flow theory prediction $\dot{\epsilon}_T/\dot{\sigma}_T = 1/E_T$ where $E_T = R^2 G$ is the transverse elastic modulus.

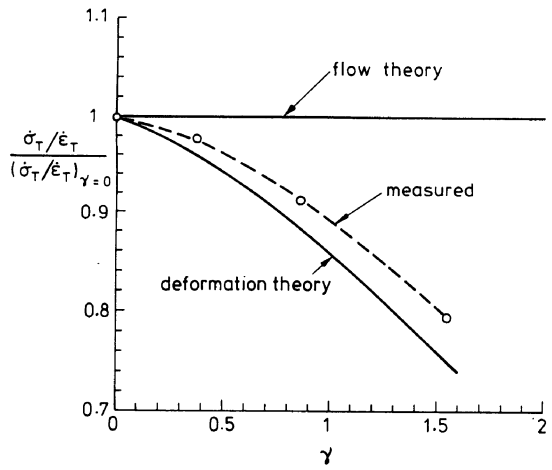

Fig. 9. Transverse tangent modulus $\dot{\sigma}_T/\dot{\epsilon}_T$ upon interruption of shear loading and application of transverse tension in the non-proportional test depicted in Fig. 8. The transverse modulus has been normalised by the initial transverse modulus for the specimen.

5. CONCLUDING REMARKS

The plasticity theory of Budiansky and Fleck [1] is adequate for capturing several aspects of the in-plane response of a carbon fibre epoxy laminate. The stress–strain response is described accurately under proportional loading, and the instantaneous modulus is predicted under non-proportional loading. Budiansky and Fleck [1] assume a deformation theory version of plasticity; this appears to be at least as accurate as a flow theory version in modelling unloading. Further work is required in order to predict damage development within the matrix and to predict the shape of the failure surfaces in stress space and in strain space.

Acknowledgements—The authors wish to thank Dr M. P. F. Sutcliffe and Professor B. Budiansky for helpful discussions. Financial support is gratefully acknowledged from the Procurement Executive of the Ministry of Defence (contract 2029/267; contract monitor Dr P. T. Curtis) and from the Office of Naval Research (contract 0014-91-J-1916, contract monitor Dr Y. D. S. Rajapakse).

REFERENCES

1. B. Budiansky and N. A. Fleck, *J. Mech. Phys. Solids* **41**, 183 (1993).
2. B. Budiansky, *J. appl. Mech.* **26**, 259 (1959).
3. I. M. Ward, *The Mechanical Behaviour of Solid Polymers*, 2nd edn. Wiley, New York (1983).
4. C. T. Sun and J. L. Chen, *J. comp. Mater.* **23**, 1009 (1989).
5. C. T. Sun and K. J. Yoon, *J. comp. Mater.* **25**, 1297 (1991).